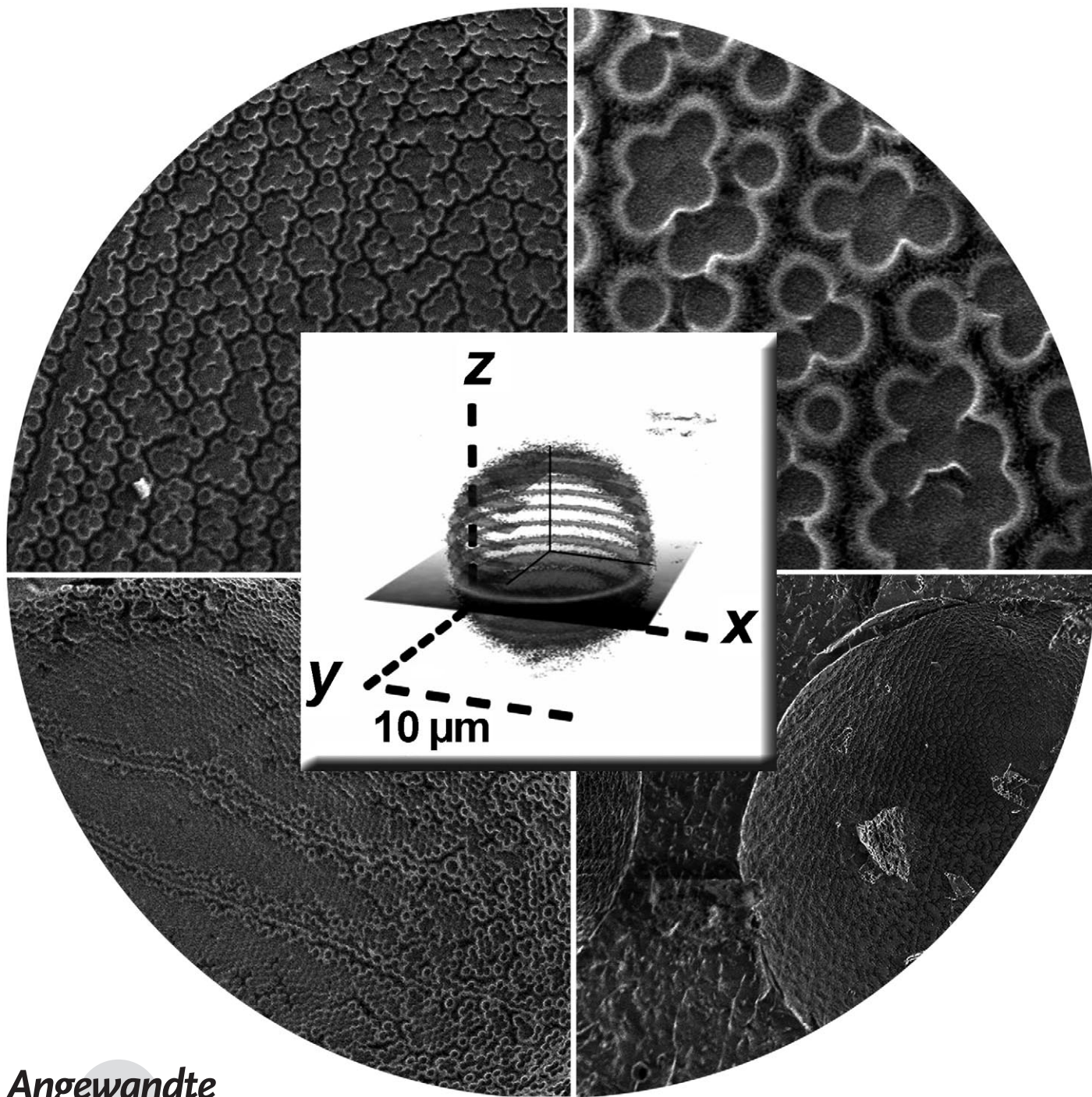


The Colloidal Suprastructure of Smart Microgels at Oil–Water Interfaces**

*Bastian Brugger, Stephan Rütten, Kim-Ho Phan, Martin Möller, and
Walter Richtering**



Emulsions are thermodynamically unstable, but can be stabilized by the addition of surfactants. In some fields, such as the oil industry, emulsions are required only in certain steps and unwanted surfactants may be present in final products.^[1] The breaking of emulsions is costly and produces a large amount of waste. Switchable low-molecular surfactants have recently sparked interest as their surface activity can be altered by appropriate stimuli, which allow controlled emulsion breaking;^[2] however, their recycling is difficult. Stabilizers based on smart particles are more promising as they can be separated easily from the product, for example, by filtration.^[3]

Particle-stabilized emulsions, or “Pickering emulsions”, were discovered by Ramsden^[4] and Pickering^[5] and can be used in, for example, separation techniques, controlled drug release, or foams, and are of both academic and industrial interest.^[6–8] A Pickering emulsion in the common sense is an emulsion that is stabilized solely by solid, mostly inorganic particles, with a diameter in the nanometer to micrometer range.^[9] The stability and type of Pickering emulsions depend on the three-phase contact angle θ , which is related to the hydrophilicity of the particles of the particles and describes the position of the particle in the oil–water interface.^[9,10] Several configurations of the particles at the interface exist, promoting stability of Pickering emulsions. The most common particle layer structure is the complete coverage of the interface by a dense particle layer. The energy required to remove an adsorbed microparticle from the interface is several orders of magnitude greater than the thermal energy kT , which makes the particle adsorption effectively irreversible, thus causing strong steric repulsion.^[9,11,12] In summary, a stable oil–water emulsion should consist of a dense layer of particles with good solubility in the continuous water phase.^[13]

The poly(*N*-isopropylacrylamide) component of soft porous poly(*N*-isopropylacrylamide)-co-(methacrylic acid) (PNIPAM-co-MAA) microgels is thermosensitive in water, and its solubility (or, in the case of microgels, swellability) in water is reduced when the temperature is higher than circa 32 °C (the volume phase transition temperature (VPTT)), which causes the microgel to shrink.^[14,15] Additionally, the incorporated MAA allows generation of internal charges at a pH value greater than 6 ($pK_a \approx 6.2$), which leads to increased osmotic pressure and thus swelling of the microgel. Recently, we demonstrated that emulsions can be stabilized solely with “smart” microgels, which are pH- and temperature-sensitive,

soft, and porous polymer particles that allow the control of emulsion stability.^[3,16] The stability of emulsions that contain these microgel stabilizers consequently depends on pH and temperature values. At high pH values ($pH > 6$) and low temperatures ($T < VPTT$), the emulsions are stable over months or even years. The oil droplets are covered by a dense monolayer of microgels (Figure 1 a). As soon as the pH value is decreased and the temperature is increased, the emulsion starts to break.^[3] The origin of the observed de-emulsification is still under discussion.

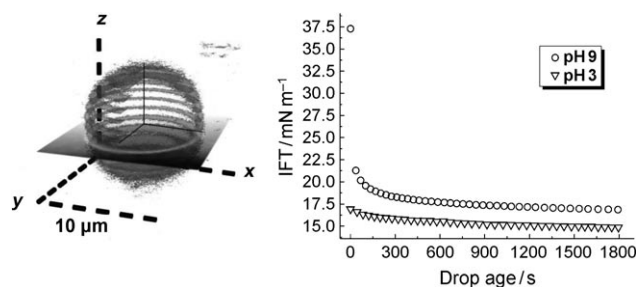


Figure 1. a) Stacked fluorescence images of a microgel-stabilized toluene droplet in water, obtained by confocal laser scanning microscopy (pH 9). The layer distance along the z-axis is 750 nm. The bright areas represent fluorescence intensity. The layer thickness was detected to be about 1 μm, which is approximately the diameter of the microgel used in this experiment. This implies that a monolayer of microgel is formed at the oil–water interface at pH 9. b) Decay of interfacial tension of a heptane–water interface as microgels adsorb. The mass fraction of microgels was 1 m% with respect to water in both experiments.

Ngai et al. have suggested that a pH- and/or temperature-driven change in the particle's polarity may cause the particles to leave the oil–water interface and thus results in emulsion destabilization, which arises from the reduced water solubility of PNIPAM when the temperature is greater than VPTT and the reduced number of charges when the pH is less than 7.^[17,18] This desorption would require the interfacial activity of the microgels to be lost, or to be at least significantly reduced, and should be easily detectable by measurements of the interfacial tension. This scenario, however, is not very likely due to the high adsorption energy of micro particles to interfaces, mentioned above.^[9,10,12] In fact, our measurements of the oil–water interfacial tension (IFT) shown in Figure 1 b reveal that the PNIPAM-co-MAA microgels do adsorb to the oil–water interfaces, independent of the pH of the microgel solution. Tsuji and Kawaguchi, however, have proposed an opposing theory of a temperature-induced contraction of the interfacial microgel layer, which leads to reduced coverage of the droplets and de-emulsification.^[19]

Surprisingly, the IFT is even lower for microgels at pH 3 (uncharged microgel) than for microgels at pH 9 (charged microgel), although the emulsions are less stable at low pH values. Obviously, the emulsion destabilization at low pH values cannot be caused by the desorption of microgels. These astonishing results were the starting point for our investigation of microgel-laden oil–water interfaces by using freeze-fraction cryo-scanning electron microscopy (cryo-SEM).

[*] B. Brugger, Prof. W. Richtering
Institute of Physical Chemistry, RWTH Aachen University
Landoltweg 2, 52056 Aachen (Germany)
Fax: (+49) 241-809-2327
E-mail: richtering@rwth-aachen.de
Homepage: <http://www.ipc.rwth-aachen.de>

S. Rütten, Dr. K.-H. Phan, Prof. M. Möller
DWI e.V. and Institute of Technical and Macromolecular Chemistry,
RWTH Aachen University
Pauwelsstr. 8, 52074 Aachen (Germany)

[**] We thank the Deutsche Forschungsgemeinschaft for financial support.

Supporting information for this article is available on the WWW under <http://dx.doi.org/10.1002/anie.200900239>.

Cryogenic electron microscopy techniques allow the characterization of shock-frozen biological and colloidal bulk samples and interfaces close to their native state.^[20–22]

Very different structures were observed in Cryo-SEM micrographs obtained from emulsion samples prepared at low and high pH values. Indeed, uncharged PNIPAM-co-MAA microgels (at pH 3) display a well-defined particle packing similar to the structure in a colloidal crystal (Figure 2). The

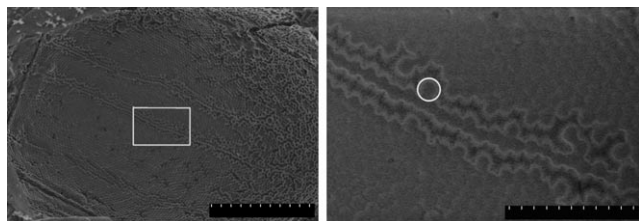


Figure 2. Cryo-SEM picture of the surface of a heptane drop covered with PNIPAM-co-MAA microgels at pH 3 at two different magnifications. The white circle in the right picture represents the hydrodynamic radius derived from dynamic light scattering (DLS) measurements of the particles. The particle sizes derived from the two techniques are similar. Scale bars: 20 μm (left image) and 5 μm (right image).

interface is fully covered by a dense layer of the uncharged microgels. However, the analogous picture of the heptane–water interface at pH 9 (Figure 3) shows a particle layer with significantly lower density, which consists of microgel clusters with uncovered areas in between. The number density of microgels is approximately twice as high for the interface covered by uncharged microgels compared to the interface covered by charged microgels (Figure 2 and Figure 3). The different particle packing appears counterintuitive, as one would expect the denser layer to be more effective in emulsion stabilization.

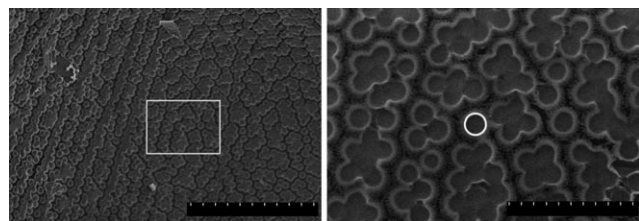


Figure 3. Cryo-SEM picture of the heptane–water interface covered with PNIPAM-co-MAA microgels at pH 9 at two different magnifications. The white circle in the right picture represents the hydrodynamic radius determined from DLS measurements of the particles. The microgel sizes appear to be bigger in the Cryo-SEM image than the sizes calculated from the DLS results. Scale bars: 20 μm (left image) and 5 μm (right image).

Pictures obtained at higher magnification show a strong linking exists between charged microgels (pH 9; see Figure 4). The oil droplets are covered by a layer of interconnected particles. At low pH values, that is, in the uncharged state, the particle density at the interface is increased, and the copolymer microgels behave similarly to pure PNIPAM

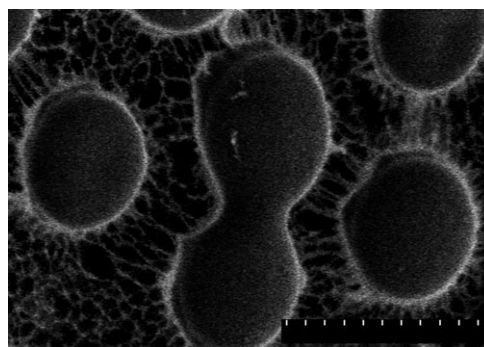


Figure 4. Cryo-SEM picture of inter-microgel connections (heptane–water interface at pH 9). Scale bar: 1 μm .

microgels, which are known to form colloidal crystals.^[23] The higher number density at the interface also leads to a stronger decrease of interfacial tension (Figure 1a). An ordered structure is formed at the oil–water interface, however, this microgel layer is not able to stabilize the emulsion.

Clusters are formed at high pH values, thus indicating a balance between attractive and repulsive forces. Currently, different concepts such as the deformation of the particle–liquid contact line and resulting capillary forces,^[24] image charges, mono-, di- and quadrupole interactions,^[25,26] as well as heterogeneity in charge distribution of the particles are discussed as the origin of interparticle attraction and repulsion at interfaces. It is difficult to deduce which of these contributions dominates, because PNIPAM-co-MAA microgels are soft, deformable particles with inhomogeneous charge distribution,^[27,28] and, furthermore, are situated at an interface of two liquids. Yet, it may be concluded that the presence of charges strongly influences the microgel behavior (compare the structures at pH 3 and 9). On a molecular scale, the deprotonation of the MAA moieties leads to local amphiphilicity that affects the chain conformation. PNIPAM chains are characterized by specific and highly cooperative hydrogen bonding patterns,^[29,30] thus local heterogeneities along dangling chains can lead, on one hand, to partial aggregation of microgels, while, on the other hand, charge interaction can lead to repulsion between clusters. The solution to this problem will certainly be a challenging task for theorists who work in this field.

The different microgel packing at the interface strongly affects emulsion stability. As the denser microgel layer, which is formed at low pH values, does not promote emulsion stability, steric repulsion between droplets cannot be the governing stabilization mechanism. At high pH values, coulomb repulsion could be contributing to emulsion stability, however, low salt sensitivity and low zeta potentials (< -10 mV) of the emulsion droplets render this stabilization mechanism rather unlikely.

Instead, we propose that the viscoelastic properties of the microgel layer are responsible for emulsion stability. Measurements carried out by using 2D interfacial dilatation rheology proved the particle layer at pH 9 to have a higher elastic modulus (about $5.5 \times 10^{-3} \text{ N m}^{-1}$) than the microgel layer at pH 3 (about $3.5 \times 10^{-3} \text{ N m}^{-1}$).^[3] This result correlates

well with the Cryo-SEM micrographs, the partially aggregated cluster structure can provide a pronounced elastic behavior whereas the dense crystalline array will lead to a brittle interface.

In conclusion, the structure of microgel packing at oil–water interfaces has been investigated by using cryo-SEM. We have presented evidence for the oil–water-interface-induced rearrangement of soft microgels, and a counterintuitive packing–emulsion stability relation for microgel-stabilized emulsions. We have shown that the structure of interfacial microgel layers strongly depends on the pH of the microgel dispersion. In contrast to previous proposals, emulsion stability is clearly not only dependent on the particle packing density.^[17,18] We have observed structural changes induced by the interface, which lead to interconnections between the individual interfacial microgels. These findings show that microgels behave quite differently at oil–water interfaces compared to solid particles used in the well-known solid-particle-stabilized Pickering emulsions.

Experimental Section

Materials: *N*-isopropylacrylamide (NIPAM, >99.0%, Acros Chemicals), methacrylic acid (MAA, >99.0%, ABCR-GmbH), *N*, *N*'-methylenebisacrylamide (BIS, >99.5%), potassium peroxodisulfate (KPS, 99.0%, Merck), *n*-heptane (>99%, Merck), toluene (>99.7%, KMF Laborchemie, Germany) and the fluorescent label methacryloxyethyl thiocarbonyl rhodamine B (MRB, Polysciences Inc.) were used as received. Doubly distilled Milli-Q-water was used in all procedures.

Microgel synthesis: This was carried out according to a previously published procedure.^[16] A three-neck flask was charged with water (1 L), which was heated to 70 °C and purged with N₂ for 1 h to remove dissolved oxygen. A solution of the monomers NIPAM, MAA, BIS, and the label MRB in degassed water was added to the previously degassed water. A solution of KPS in degassed water was added to the monomer solution, which was then mechanically stirred (the overhead stirrer was set to a speed of 350 rpm). After 5 h, the reaction mixture was cooled to room temperature under constant stirring. After filtration through glass wool, the mixture was centrifuged at 50000 rpm for 40 min and redispersed three times in doubly distilled water. After these cleaning steps, the microgels were freeze dried. The microgels were redispersed in doubly distilled water for 4–5 days prior to use in experiments. The characterization of the microgels used in this study can be found in the Supporting Information.

Preparation of Cryo-SEM samples: The pH-adjusted microgel solution and heptane were combined. After shaking the sample and equilibration of the interface for a minimum of 1 h, a drop of the emulsion was transferred into a copper tube in such a way that an excess of the emulsion formed a drop on top of the tube. The sample was frozen in liquid nitrogen and transferred into the cooled sample chamber ($T = -140$ °C, $p = 10^{-6}$ Pa). There, the drop on top of the tip was broken away with a razor blade. The temperature in the chamber was raised to -90 °C to create a clean surface. After 5 to 10 min, the temperature was reduced again and the sample was transferred directly into the microscope. The cryo-SEM images were taken with a Hitachi S-4800 electron microscope equipped with a liquid-nitrogen-cooled sample preparation and transfer unit.

Confocal fluorescence imaging: The confocal laser scanning microscopy pictures were taken on a MicroTime200 (PicoQuant GmbH, Berlin, Germany). A laser with a wavelength of 531–533 nm was used to excite the fluorescent label on the microgel. The emitted light was detected by single avalanche photo diodes (SPAD, Micro Photon Devices, Bolzano, Italy). The emulsion was placed on the

sample glass and a series of *x/y* layers was scanned. The temperature was 23 °C and the *Z* distance between the layers was 750 nm.

Interfacial tension (IFT) measurements: A video-enhanced pendant drop setup (DSA100, Krüss, Germany) was used. A drop of water–microgel dispersion was created in a cuvette filled with the oil. The interfacial tension was derived from the drop shape and the density difference of the liquids. The IFT data were recorded from the live image with one reading every 1–2 s. The number of data points has been reduced for display in the graphs.

Received: January 14, 2009

Published online: March 27, 2009

Keywords: copolymerization · de-emulsification · emulsions · gels · interfaces

- [1] D. Langevin, S. Poteau, I. Henaut, J. F. Argillier, *Oil Gas Sci. Technol.* **2004**, 59, 511.
- [2] Y. Liu, P. G. Jessop, M. Cunningham, C. A. Eckert, C. L. Liotta, *Science* **2006**, 313, 958.
- [3] B. Brugger, B. A. Rosen, W. Richtering, *Langmuir* **2008**, 24, 12202.
- [4] W. Ramsden, *Proc. R. Soc. London* **1903**, 72, 156.
- [5] S. U. Pickering, *J. Chem. Soc.* **1907**, 91, 2001.
- [6] I. G. Loscertales, A. Barrero, I. Guerrero, R. Cortijo, M. Marquez, A. M. Ganan-Calvo, *Science* **2002**, 295, 1695.
- [7] A. D. Dinsmore, M. F. Hsu, M. G. Nikolaides, M. Marquez, A. R. Bausch, D. A. Weitz, *Science* **2002**, 298, 1006.
- [8] B. P. Binks, R. Murakami, *Nat. Mater.* **2006**, 5, 865.
- [9] B. P. Binks, *Curr. Opin. Colloid Interface Sci.* **2002**, 7, 21.
- [10] R. Aveyard, J. H. Clint, T. S. Horozov, *Phys. Chem. Chem. Phys.* **2003**, 5, 2398.
- [11] R. Aveyard, J. H. Clint, D. Nees, *Colloid Polym. Sci.* **2000**, 278, 155.
- [12] F. Reincke, W. K. Kegel, H. Zhang, M. Nolte, D. Wang, D. Vanmaekelbergh, H. Möhwald, *Phys. Chem. Chem. Phys.* **2006**, 8, 3828.
- [13] S. Melle, M. Lask, G. G. Fuller, *Langmuir* **2005**, 21, 2158.
- [14] R. H. Pelton, *Adv. Colloid Interface Sci.* **2000**, 85, 1.
- [15] R. H. Pelton, P. Chibante, *Colloids Surf.* **1986**, 20, 247.
- [16] B. Brugger, W. Richtering, *Langmuir* **2008**, 24, 7769.
- [17] T. Ngai, S. H. Behrens, H. Auweter, *Chem. Commun.* **2005**, 331.
- [18] T. Ngai, S. H. Behrens, H. Auweter, *Macromolecules* **2006**, 39, 8171.
- [19] S. Tsuji, H. Kawaguchi, *Langmuir* **2008**, 24, 3300.
- [20] H. Fernández-Morán, *Ann. N. Y. Acad. Sci.* **1960**, 85, 689.
- [21] M. Adrian, J. Dubochet, J. Lepault, A. W. McDowell, *Nature* **1984**, 308, 32.
- [22] H. Luo, L. E. Scriven, L. F. Francis, *J. Colloid Interface Sci.* **2007**, 316, 500.
- [23] H. Senff, W. Richtering, *J. Chem. Phys.* **1999**, 111, 1705.
- [24] J. Lucassen, *Colloids Surf.* **1992**, 65, 131.
- [25] K. D. Danov, P. A. Krachevsky, B. N. Naydenov, G. Brenn, *J. Colloid Interface Sci.* **2005**, 287, 121.
- [26] M. E. Leunissen, A. van Blaaderen, A. D. Hollingsworth, M. T. Sullivan, P. M. Chaikin, *Proc. Natl. Acad. Sci. USA* **2007**, 104, 2585.
- [27] M. Stieger, W. Richtering, J. S. Pedersen, P. Lindner, *J. Chem. Phys.* **2004**, 120, 13.
- [28] B. H. Tan, K. C. Tam, *Adv. Colloid Interface Sci.* **2008**, 136, 25.
- [29] M. Keerl, V. Smirnovas, R. Winter, W. Richtering, *Angew. Chem.* **2008**, 120, 344; *Angew. Chem. Int. Ed.* **2008**, 47, 338.
- [30] F. Tanaka, T. Koga, F. W. Winnik, *Phys. Rev. Lett.* **2008**, 101, 028302.